

ELECTRONIC SUPPLEMENTARY INFORMATION

Sensitization experiments of ultrasmall gold nanoclusters: determination of triplet quantum yields and molar absorption coefficients

Hayato Sakai,^a Sunao Hiramatsu,^a Aoi Akiyama,^b Yuichi Negishi,^{*bc} and Taku Hasobe^{*a}

^aDepartment of Chemistry, Faculty of Science and Technology, Keio University,
Yokohama, Kanagawa 223-8522, Japan

^bDepartment of Applied Chemistry, Faculty of Science, Tokyo University of Science, 1-
3 Kagurazaka, Shinjuku-ku, Tokyo 162-8601, Japan

^cInstitute of Multidisciplinary Research for Advanced Materials, Tohoku University,
Katahira 2-1-1, Aoba-ku, Sendai 980-8577, Japan

Experimental section

General and materials. All solvents and reagents of the best grade available were purchased from commercial suppliers such as Tokyo Chemical Industry, Kanto Chemical Co., Inc., Nacalai Tesque, and FUJIFILM Wako Pure Chemical Corporation. All commercial reagents were used without further purification. Column flash chromatography was performed on silica gel (Fuji Silysia Chemical LTD., 40-50 mm or 100-210 mm). ^1H NMR and ^{13}C NMR spectra were recorded on a JEOL ECX-400, AL-400, or ALPHA-400 spectrometer using the solvent peak as the reference standard, with chemical shifts given in parts per million. CDCl_3 were used as NMR solvent. MALDI-TOF mass spectra were recorded on Shimadzu MALDI-7090.

Spectroscopic measurements. UV-VIS absorption spectra were recorded on Agilent (8453) UV-VIS-NIR spectrophotometer. Fluorescence spectra were recorded on JASCO (FP-8500) spectrofluorophotometer. NIR emission spectra are recorded on Horiba Jobin Yvon FluoroMax Plus spectrofluorometer equipped with NIR-PMT unit: Hamamatsu Photonics H10330B-75.

Nanosecond laser flash photolysis. Nanosecond transient absorption measurements were carried out using Unisoku TSP-2000 flash spectrometer. Surelite-I Nd-YAG (Q-switched) laser was employed for the flash photo-irradiation. A 150 W Xenon arc and halogen lamps were used as the monitor light source.

Picosecond Transient Absorption Measurement.¹ Picosecond transient absorption measurement was conducted by the device made by Unisoku Co., Ltd. Measurement method used in this measurement was Randomly Interleaved Pulse Train Method. Temperature-dependent measurements were performed by using CoolSpek USP-203-SH-ST (Unisoku Co., Ltd).

Femtosecond pump-probe system. The transient absorption spectroscopy measurements were carried out using a home-made femtosecond pump-probe system. Yb laser (PHAROS PH2-10W, Light Conversion) was used to create fundamental light pulses at 1030 nm at a repetition rate of 1 kHz. The pulse energy was 200 μJ , and the pulse duration was approximately 290 fs. 65% of the fundamental beam was directed to ORPHEUS optical parametric amplifier (Light Conversion) to produce excitation pulses at the desired wavelength or utilized to generate SHG (515 nm) and THG (343 nm) for sample pumping. The rest of the beam was delivered to a delay stage then attenuated

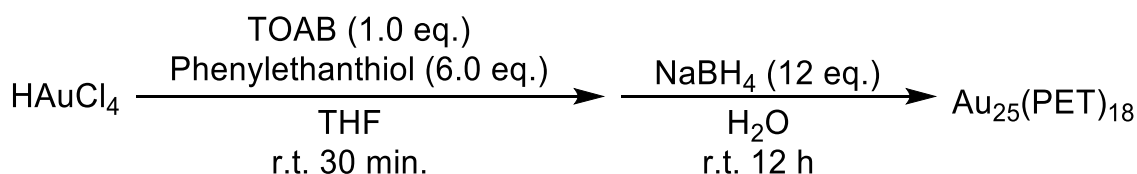
appropriately and focused onto liquid D₂O or a sapphire crystal to generate a stable white light continuum for sample probing. The probe light was introduced to polychromators equipped with a CMOS array (USP-PSMM-PK120, Unisoku) for the visible part of the spectrum and an InGaAs diode array (USP-NIR-PDA256, Unisoku) for the near-infrared (NIR) wavelengths. The measurements were carried out by comparing responses with and without excitation using a chopper synchronized with the fundamental laser pulses. The spectra were typically acquired by recording 2000 shots, that is, averaging over 2 s. Excitation energies were sufficiently lowered to avoid multiple exciton generation; this was verified by recording a series of measurements with different excitation energies for the same sample. No excitation energy dependence of the response was observed. Temperature-dependent measurements were performed by using CoolSpek USP-203-SH-ST (Unisoku Co., Ltd).

Global and target analysis.² Global (singular value decomposition-based) and target (differential equation-based) analysis is accomplished using the Glotaran software package (<http://glotaran.org>).

Synthesis.

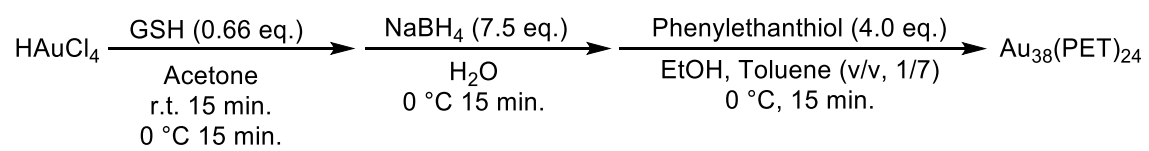
Au₂₅(PET)₁₈³⁻: HAuCl₄ and TOAB (TOA⁺Br⁻) (1.0 eq.) firstly added to the THF solution and stirred for 15 min. Phenylethanethiol (6.0 eq.) was then added at room temperature. The solution was stirred for 30 min. until it was completely colorless (in this process, the Au(I)SR polymeric intermediates were completely synthesized). After that, NaBH₄ (12 eq.) dissolved in room temperature water was then rapidly added to the THF solution. The reaction was allowed to quietly stir for more than 12 h, and then the obtained solution was filtered and evaporated to get the crude product. The toluene extract was washed several times with copious amounts methanol to get the pure [TOA⁺][Au₂₅(S-C₂H₄Ph)₁₈]⁻.

Scheme S1. Synthesis of Au₂₅(PET)₁₈



Au₃₈(PET)₂₄⁴⁻: HAuCl₄ (1.00 mmol) and GSH powder (0.658 mmol) were mixed in 30 mL of acetone at room temperature under vigorous stirring for 15 min. The mixture (yellowish cloudy suspension) was then cooled to 0 °C in an ice bath. After 15 min, a solution of NaBH₄ (7.53 mmol) was rapidly added to the suspension under vigorous stirring. The color of the solution immediately turned black after addition of NaBH₄, indicating the formation of Au nanoclusters. After 15 min, the black Au_n(SG)_m nanoclusters were found to precipitate out and stick to the inner wall of the flask. The clear acetone solution was decanted and 12 mL of water was added to dissolve the Au_n(SG)_m clusters. A solution of Au_n(SG)_m (dissolved in 12 mL of nano-pure water) was mixed with 0.6 mL of ethanol, 4 mL of toluene, and phenylethanethiol (3.92 mmol). Here, ethanol is added to prompt the phase transfer of Au_n(SG)_m from water to organic phase. The diphasic solution was heated to and maintained at 80 °C under air atmosphere, the Au_n(SG)_m clusters were found to transfer from the water phase to the organic phase in less than 10 min. The thermal process was allowed to continue 40 h at 80 °C. Over the long-time etching process, the initial polydisperse Au_n nanoclusters were finally converted to monodisperse Au₃₈(PET)₂₄ clusters. The organic phase was thoroughly washed with methanol to remove excess thiol. Then the Au₃₈(PET)₂₄ nanoclusters were simply separated from Au(I)-SG by extraction with toluene.

Scheme S2. Synthesis of $\text{Au}_{38}(\text{PET})_{24}$



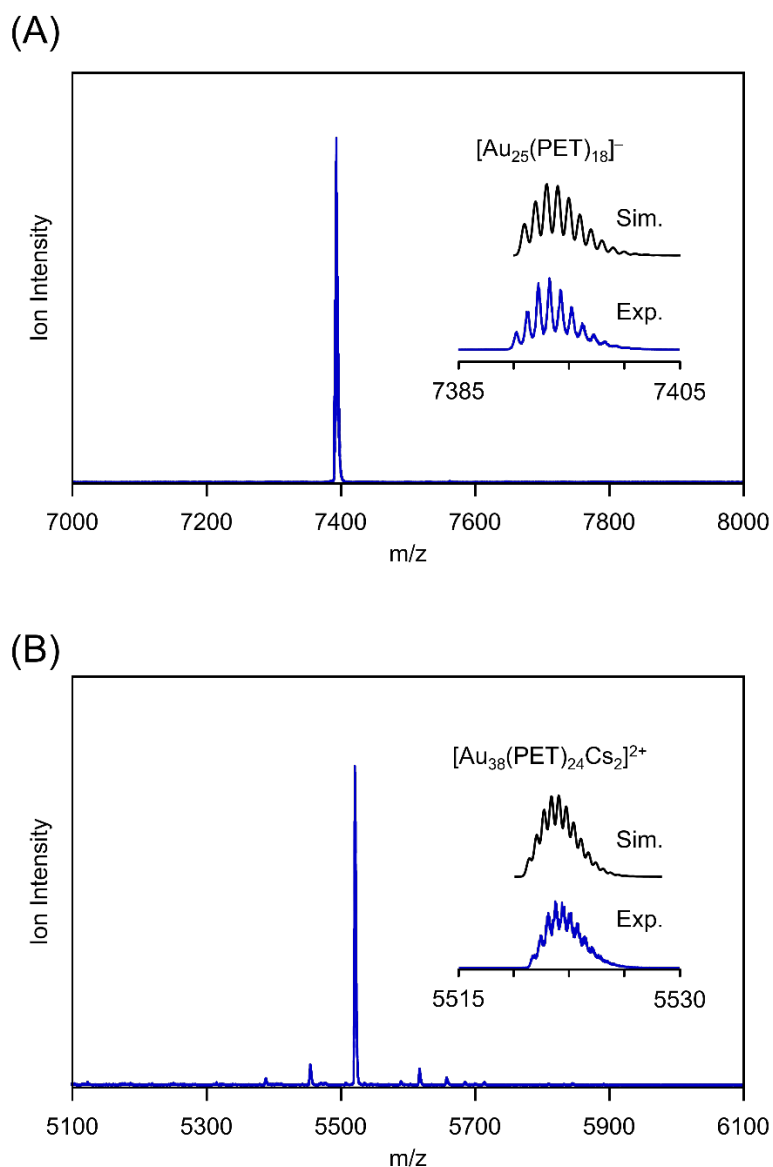


Fig. S1 ESI mass spectra of (A) $\text{Au}_{25}(\text{PET})_{18}$ in the negative mode and (B) $\text{Au}_{38}(\text{PET})_{24}$ in the positive mode. Inset: The measured (blue trace) and simulated (black trace) isotopic patterns of (A) $[\text{Au}_{25}(\text{PET})_{18}]^{-}$ and (B) $[\text{Au}_{38}(\text{PET})_{24}\text{Cs}_2]^{2+}$, respectively. Since $[\text{Au}_{25}(\text{PET})_{18}]^{-}$ is a negative ion, it was observed in negative ion mode. In contrast, $[\text{Au}_{38}(\text{PET})_{24}]^0$ is neutral, so Cs^{2+} was added as a cation source in solution and observed in positive ion mode. As a result, $[\text{Au}_{38}(\text{PET})_{24}]^0$ was observed as $[\text{Au}_{38}(\text{PET})_{24}\text{Cs}_2]^{2+}$. Both $[\text{Au}_{25}(\text{PET})_{18}]^{-}$ and $[\text{Au}_{38}(\text{PET})_{24}\text{Cs}_2]^{2+}$ peak positions were in very good agreement with the molecular weights of $[\text{Au}_{25}(\text{PET})_{18}]^{-}$ and $[\text{Au}_{38}(\text{PET})_{24}\text{Cs}_2]^{2+}$ (see: the comparison of isotopic distribution with simulations). In addition, little was observed in the mass spectrum except for the sample peaks. These results strongly confirm that $\text{Au}_{25}(\text{PET})_{18}$ and $\text{Au}_{38}(\text{PET})_{24}$ used in this study are highly pure samples. Moreover, in the case of

$\text{Au}_{25}(\text{PET})_{18}$, the mass peak appeared in mass spectrum cannot be explained by the combinations of the number of Au and PET except $\text{Au}_{25}(\text{PET})_{18}$ (see: Table S1).

Table S1. Possible combinations of metal (Au) and thiolate (PET) matching the molecular weight of the main peak observed in the ESI-MS of $\text{Au}_{25}(\text{PET})_{18}$ (see: Fig. S1A in ESI).

Chemical Composition	Calculated molecular weight ^a	Difference in exp. and calc. peak values
(PET) ₅₃	7272.8	-120.4
Au(PET) ₅₂	7332.5	-60.7
Au ₂ (PET) ₅₁	7392.3	-0.9
Au ₃ (PET) ₅₀	7452.0	58.8
Au ₄ (PET) ₄₈	7374.5	-18.7
Au ₅ (PET) ₄₇	7434.3	41.1
Au ₆ (PET) ₄₅	7356.8	-36.4
Au ₇ (PET) ₄₄	7416.5	23.3
Au ₈ (PET) ₄₂	7339.1	-54.1
Au ₉ (PET) ₄₁	7398.8	5.6
Au ₁₀ (PET) ₄₀	7458.5	65.3
Au ₁₁ (PET) ₃₈	7381.1	-12.1
Au ₁₂ (PET) ₃₇	7440.8	47.6
Au ₁₃ (PET) ₃₅	7363.3	-29.9
Au ₁₄ (PET) ₃₄	7423.1	29.9
Au ₁₅ (PET) ₃₂	7345.6	-47.6
Au ₁₆ (PET) ₃₁	7405.3	12.1
Au ₁₇ (PET) ₂₉	7327.9	-65.3
Au ₁₈ (PET) ₂₈	7387.6	-5.6
Au ₁₉ (PET) ₂₇	7447.4	54.2
Au ₂₀ (PET) ₂₅	7369.9	-23.3
Au ₂₁ (PET) ₂₄	7429.6	36.4
Au ₂₂ (PET) ₂₂	7352.1	-41.1
Au ₂₃ (PET) ₂₁	7411.9	18.7
Au ₂₄ (PET) ₁₉	7334.4	-58.8
Au₂₅(PET)₁₈	7394.2	1.0
Au ₂₆ (PET) ₁₇	7453.9	60.7
Au ₂₇ (PET) ₁₅	7376.4	-16.8
Au ₂₈ (PET) ₁₄	7436.2	43.0
Au ₂₉ (PET) ₁₂	7358.7	-34.5
Au ₃₀ (PET) ₁₁	7418.4	25.2
Au ₃₁ (PET) ₉	7341.0	-52.2
Au ₃₂ (PET) ₈	7400.7	7.5
Au ₃₃ (PET) ₇	7460.5	67.3
Au ₃₄ (PET) ₅	7383.0	-10.2
Au ₃₅ (PET) ₄	7442.7	49.5
Au ₃₆ (PET) ₂	7365.2	-28.0
Au ₃₇ (PET)	7425.0	31.8
Au ₃₈	7484.7	91.5

^aCalculated molecular weight. This is different from the peak top of the isotope pattern. The peak top of the isotope pattern of $\text{Au}_{25}(\text{PET})_{18}$ is 7393 which is well consistent with the observed peak top ($m/z = 7393.2$).

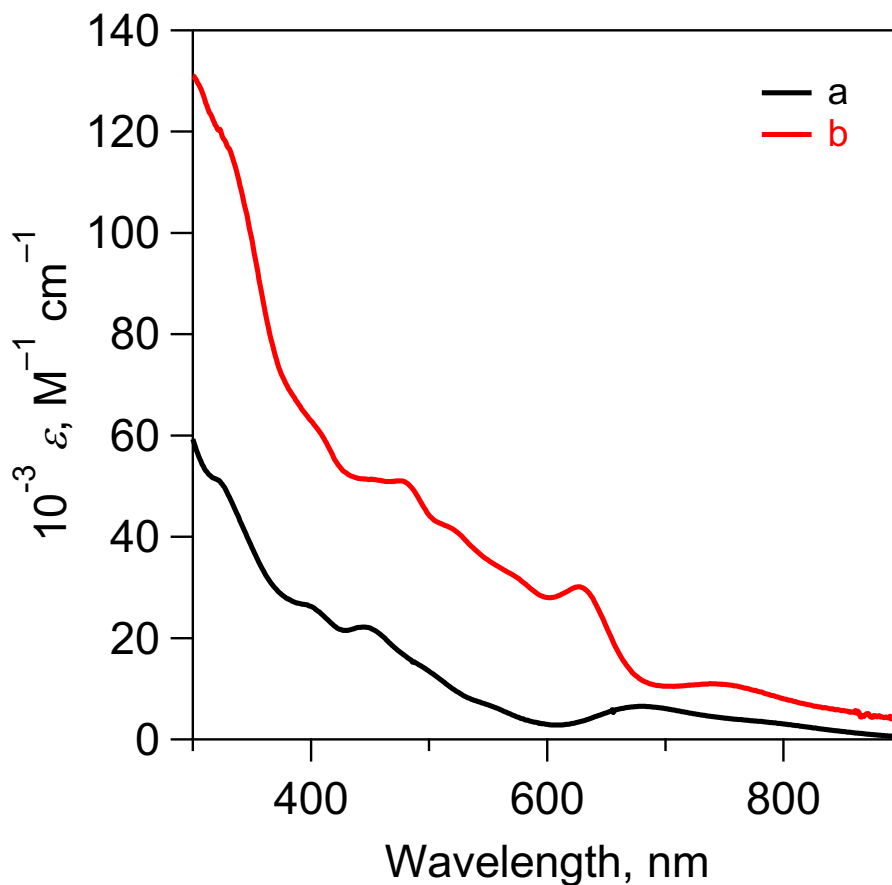


Fig. S2 Absorption spectra of (a) Au₂₅(PET)₁₈ (black) and (b) Au₃₈(PET)₂₄ (red) in toluene. Measurements were performed at room temperature (298 K). These absorption spectra well reproduced the reported spectra such as Au₂₅(PET)₁₈⁵ and Au₃₈(PET)₂₄⁴, indicating that these gold nanoclusters have the same chemical formulas and geometric structures as previously reported (see: the above reference papers (refs. 4 and 5)).

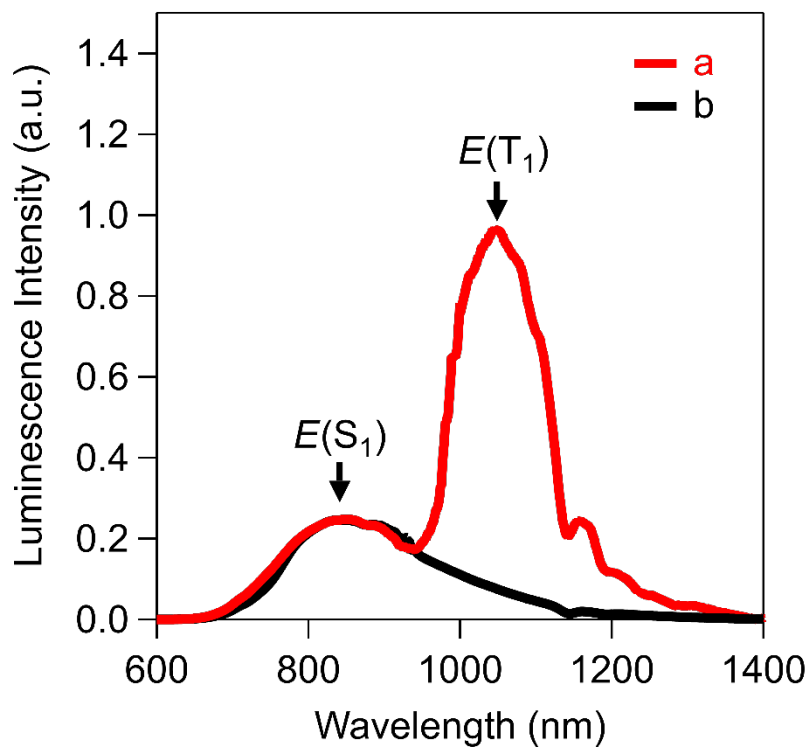


Fig. S3 Luminescence spectra of Au₂₅(PET)₁₈ in (a) Ar-saturated toluene (red) and (b) O₂-saturated toluene (black) at 83 K ($\lambda_{\text{ex}} = 335$ nm). The significant quenching trend of the low-energy band by O₂ relative to the high-energy band demonstrates the phosphorescent emission derived from ³Au₂₅(PET)₁₈*. The resulting $E(S_1)$ and $E(T_1)$ of Au₂₅(PET)₁₈ were thus determined to be 1.5 eV and 1.2 eV, respectively. These values are comparable to the previous report.⁶

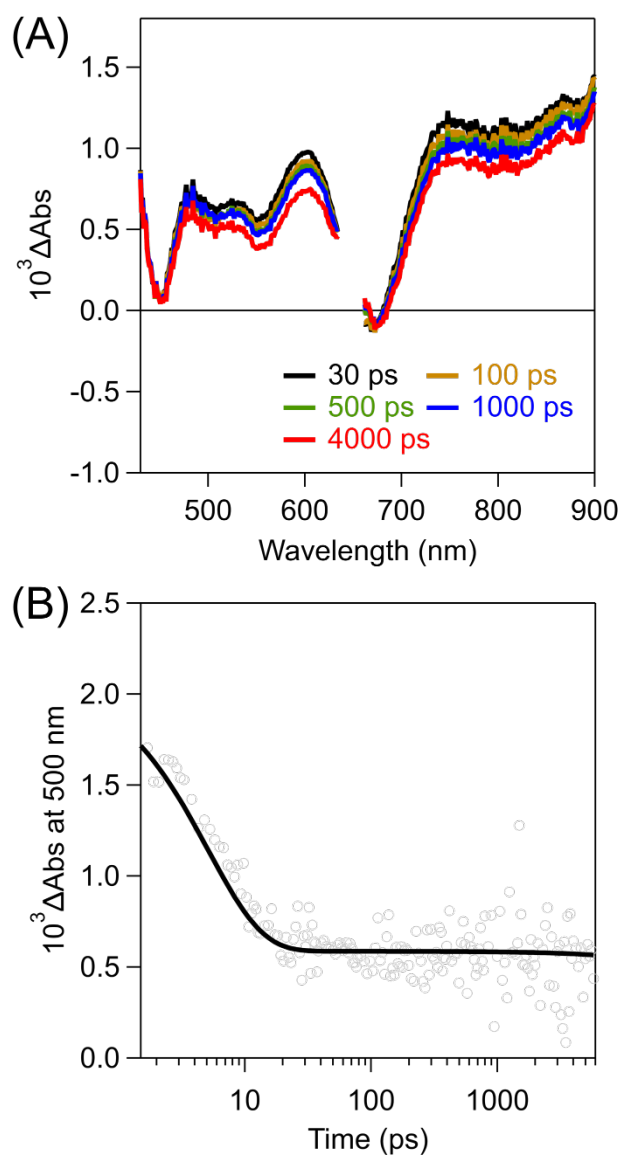


Fig. S4 (A) Femtosecond transient absorption spectra (fs-TAS) of Au₂₅(PET)₁₈ in toluene ($\lambda_{\text{ex}} = 650$ nm) (time range from 0 to 6000 ps). (B) The corresponding time profile of fs-TAS of Au₂₅(PET)₁₈ at 500 nm. Measurements were performed at room temperature (298 K).

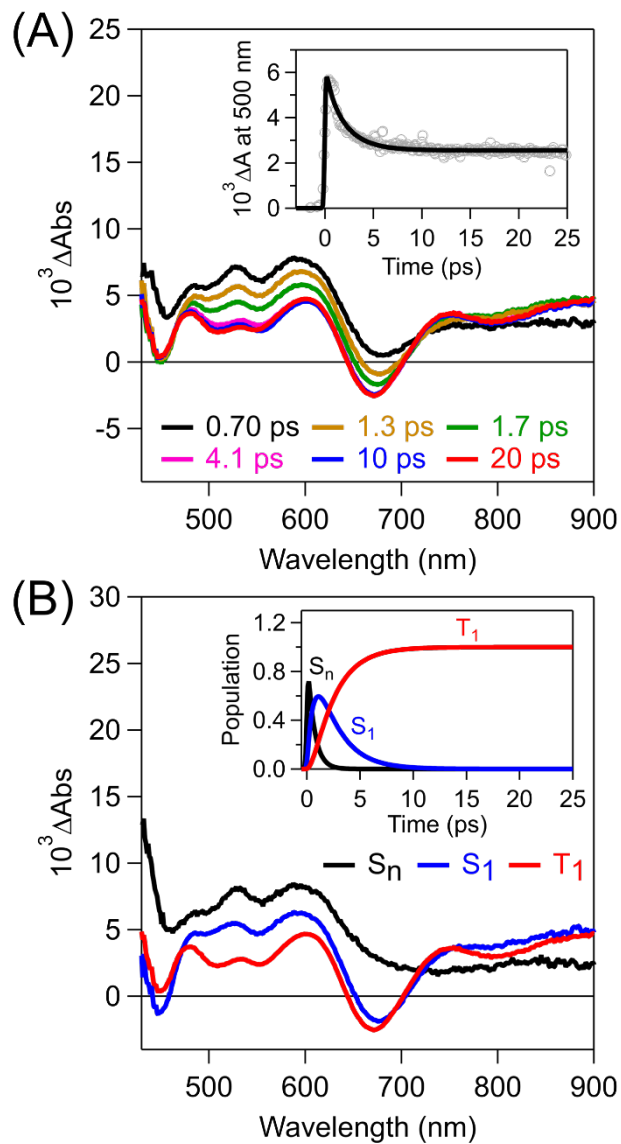


Fig. S5 (A) Femtosecond transient absorption spectra (fs-TAS) of $\text{Au}_{25}(\text{PET})_{18}$ in toluene ($\lambda_{\text{ex}} = 350 \text{ nm}$) (time range from 0 to 25 ps). The inset shows the time profile at 500 nm. (B) Corresponding species-associated spectra (SAS) of the higher singlet excited state: S_n (black), S_1 (blue) and T_1 (red). The inset shows the time-dependent concentration profiles of the higher singlet excited state: S_n (black), S_1 (blue) and T_1 (red). Measurements were performed at room temperature (298 K).

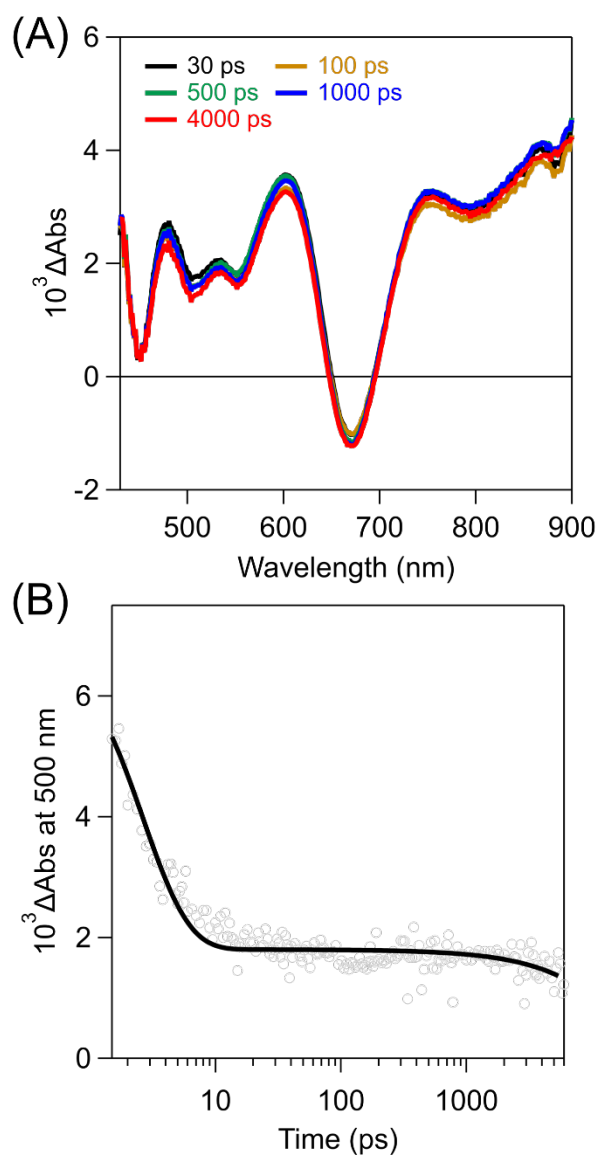


Fig. S6 (A) Femtosecond transient absorption spectra (fs-TAS) of Au₂₅(PET)₁₈ in toluene ($\lambda_{\text{ex}} = 350$ nm) (time range from 0 to 6000 ps). (B) The corresponding time profile of fs-TAS at 500 nm. Measurements were performed at room temperature (298 K).

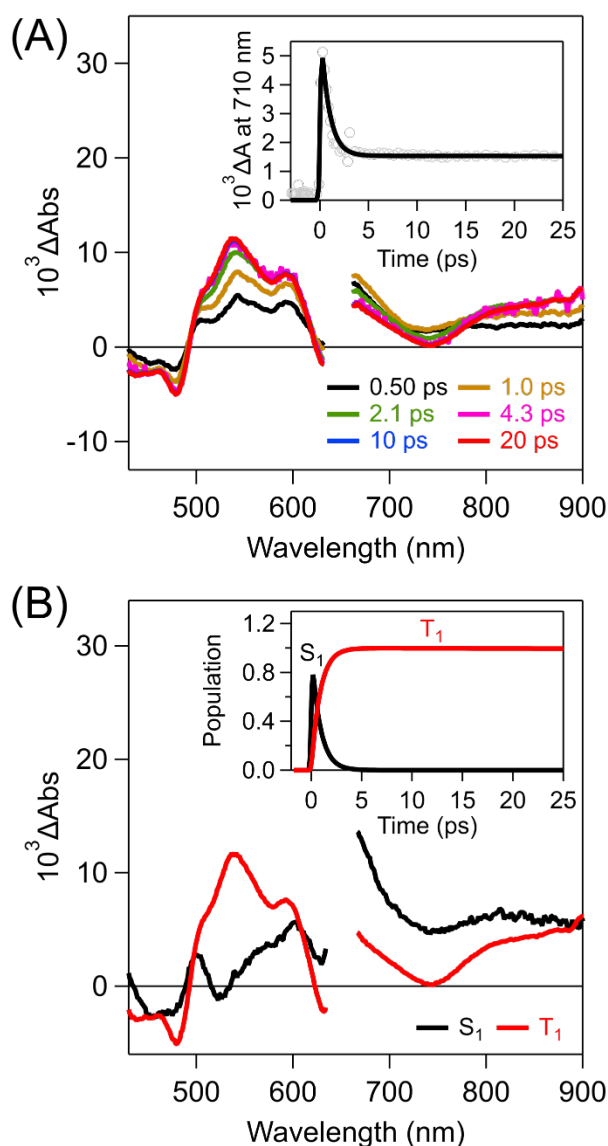


Fig. S7 (A) Femtosecond transient absorption spectra (fs-TAS) of $\text{Au}_{38}(\text{PET})_{24}$ in toluene ($\lambda_{\text{ex}} = 650 \text{ nm}$) (time range from 0 to 25 ps). The inset shows the time profile at 710 nm. (B) Corresponding species-associated spectra (SAS) of S_1 (black) and T_1 (red). The inset shows the time-dependent concentration profiles of S_1 (black) and T_1 (red). Measurements were performed at room temperature (298 K).

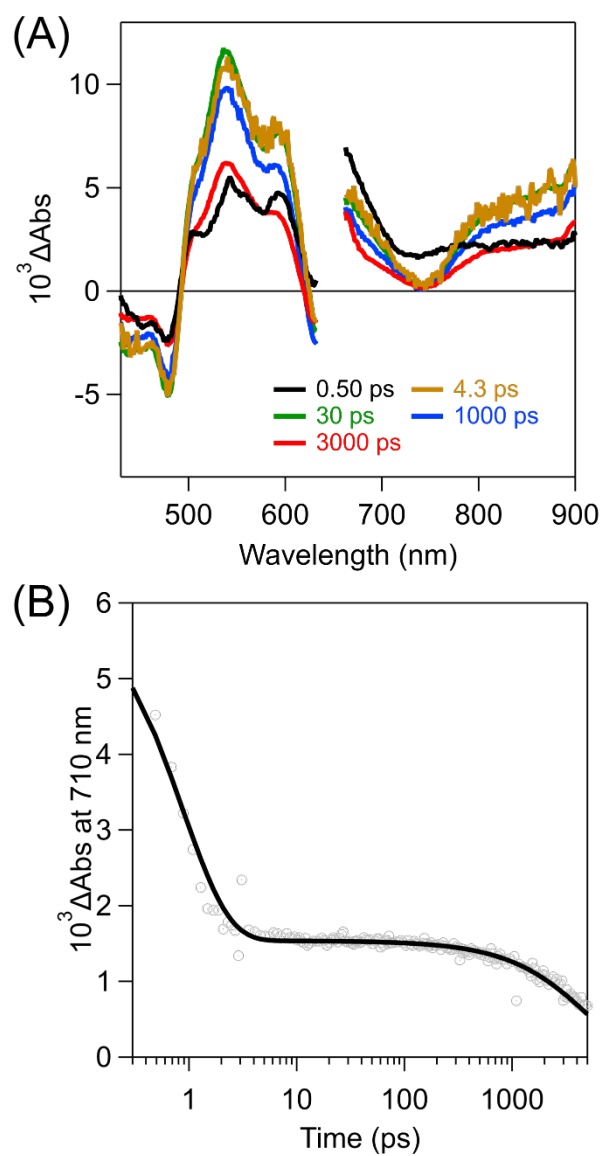


Fig. S8 (A) Femtosecond transient absorption spectra (fs-TAS) of Au₃₈(PET)₂₄ in toluene ($\lambda_{\text{ex}} = 650$ nm) (time range from 0 to 6000 ps). (B) The corresponding time profile of fs-TAS at 710 nm. Measurements were performed at room temperature (298 K).

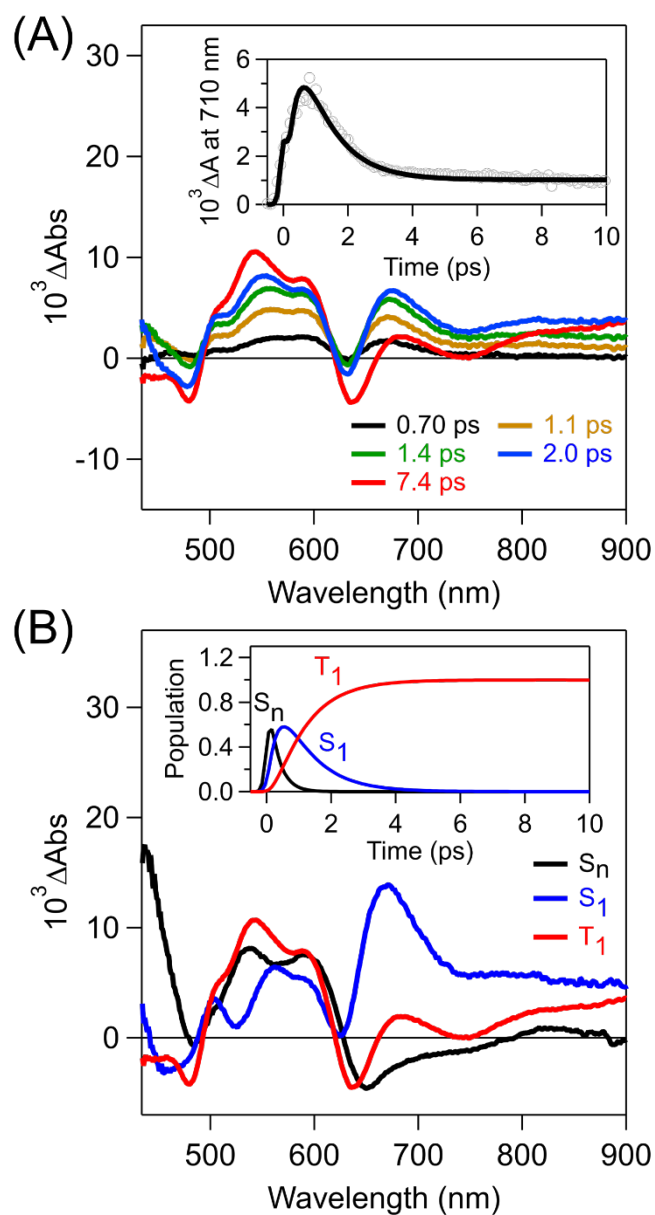


Fig. S9 (A) Femtosecond transient absorption spectra (fs-TAS) of $\text{Au}_{38}(\text{PET})_{24}$ in toluene ($\lambda_{\text{ex}} = 350 \text{ nm}$) (time range from 0 to 10 ps). The inset shows the time profile at 710 nm. (B) Corresponding species-associated spectra (SAS) of the higher singlet excited state: S_n (black), S_1 (blue) and T_1 (red). The inset shows the time-dependent concentration profiles of the higher singlet excited state: S_n (black), S_1 (blue) and T_1 (red). Measurements were performed at room temperature (298 K).

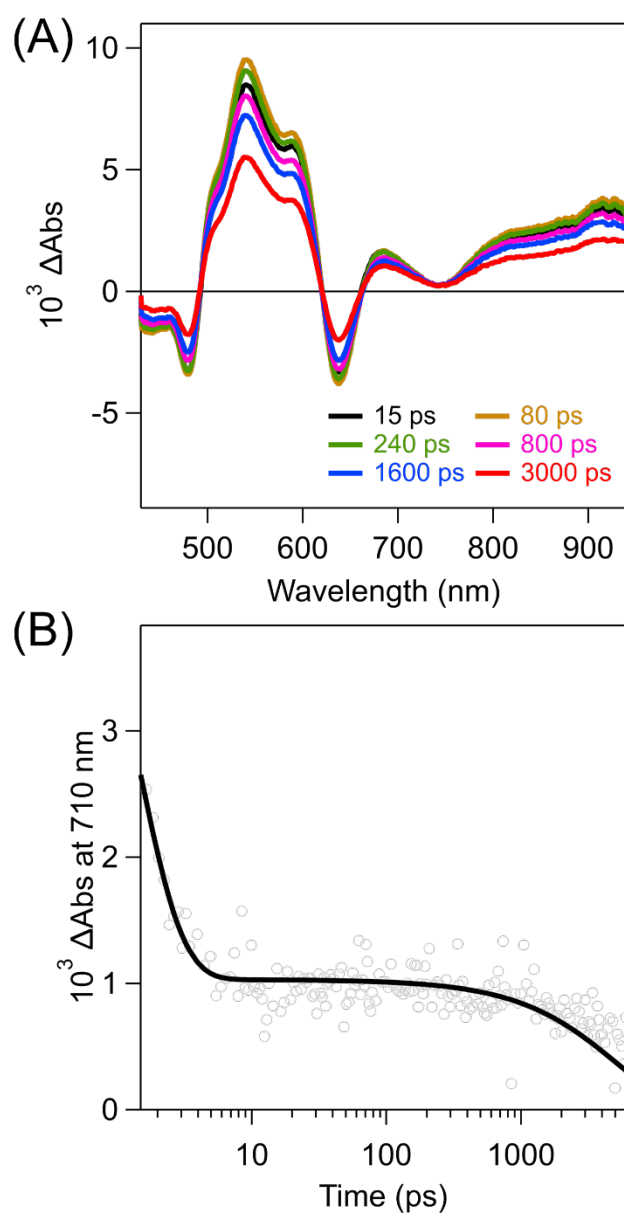


Fig. S10 (A) Femtosecond transient absorption spectra (fs-TAS) of $\text{Au}_{38}(\text{PET})_{24}$ in toluene ($\lambda_{\text{ex}} = 350 \text{ nm}$) (time range from 0 to 6000 ps). (B) The corresponding time profile of fs-TAS of $\text{Au}_{38}(\text{PET})_{24}$ at 710 nm. Measurements were performed at room temperature (298 K).

Kinetic analysis methods

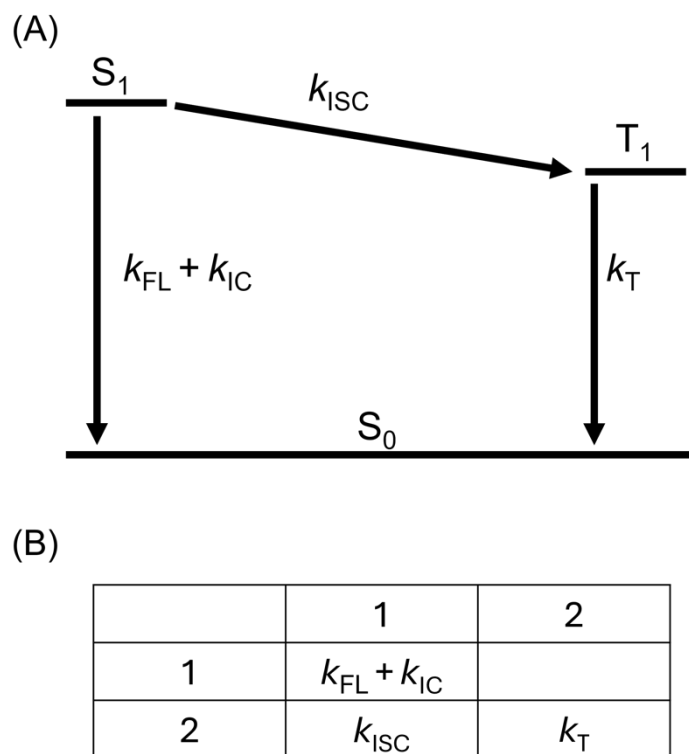
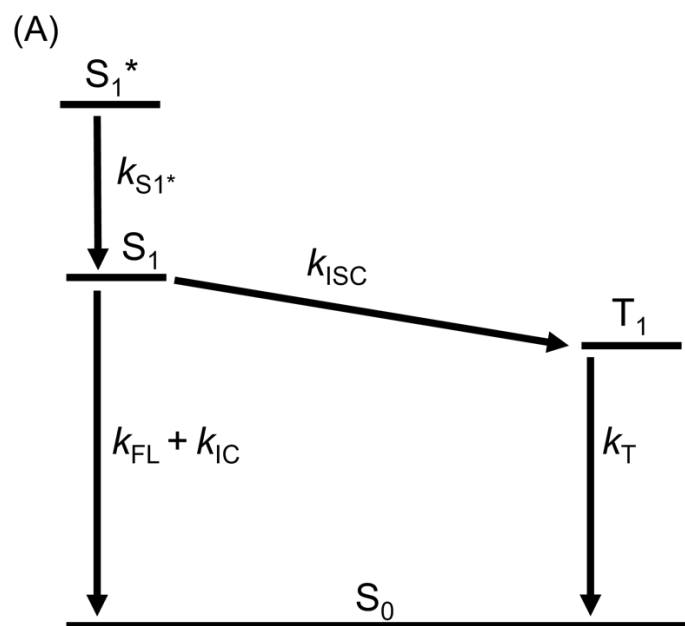


Fig. S11 (A) A kinetic scheme of $\text{Au}_{25}(\text{PET})_{18}$ and $\text{Au}_{38}(\text{PET})_{24}$ ($\lambda_{\text{ex}} = 650 \text{ nm}$) and (B) k -matrices for target analysis by using Glotaran.²



(B)

	1	2	3
1			
2	k_{S1^*}	$k_{FL} + k_{IC}$	
3		k_{ISC}	k_T

Fig. S12 (A) A kinetic scheme of $Au_{25}(PET)_{18}$ and $Au_{38}(PET)_{24}$ ($\lambda_{ex} = 350$ nm) and (B) k -matrices for target analysis by using Glotaran.²

All k -matrices for target analysis were arranged based on the kinetic schemes, and kinetic analyses were performed by Glotaran using the k -matrices. For the others, lifetimes and rate constants were estimated by single-exponential or double exponential fitting to the decay curves of TAS.

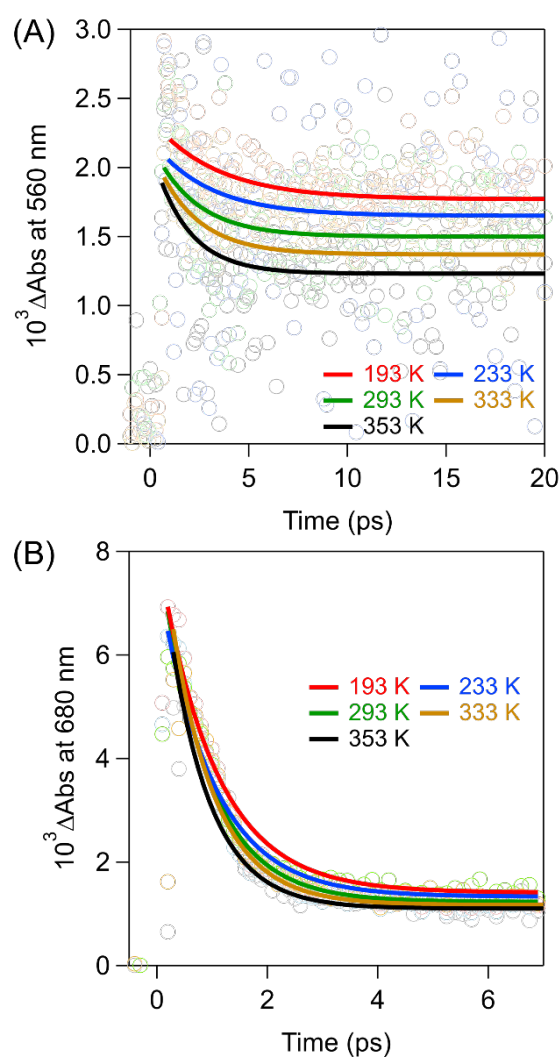


Fig. S13 (A) Temperature-dependent time profiles of $\text{Au}_{25}(\text{PET})_{18}$ at 560 nm in toluene using femtosecond transient absorption measurements ($\lambda_{\text{ex}} = 650 \text{ nm}$). (B) Temperature-dependent time profiles of $\text{Au}_{38}(\text{PET})_{24}$ at 680 nm in toluene at different temperatures using femtosecond transient absorption measurements ($\lambda_{\text{ex}} = 650 \text{ nm}$). Although there were no differences in the changes in the spectral shapes from S_1 to T_1 with varying temperature, the decay rate constants of S_1 gradually increased with increasing temperature. This is mainly due to the contribution of the non-radiative deactivation process caused by the vibrational structures of the ligand-protected metal nanoclusters. Therefore, there are no transition processes from T_1 to S_1 (reverse intersystem crossing: RISC) for $\text{Au}_{25}(\text{PET})_{18}$ and $\text{Au}_{38}(\text{PET})_{24}$.

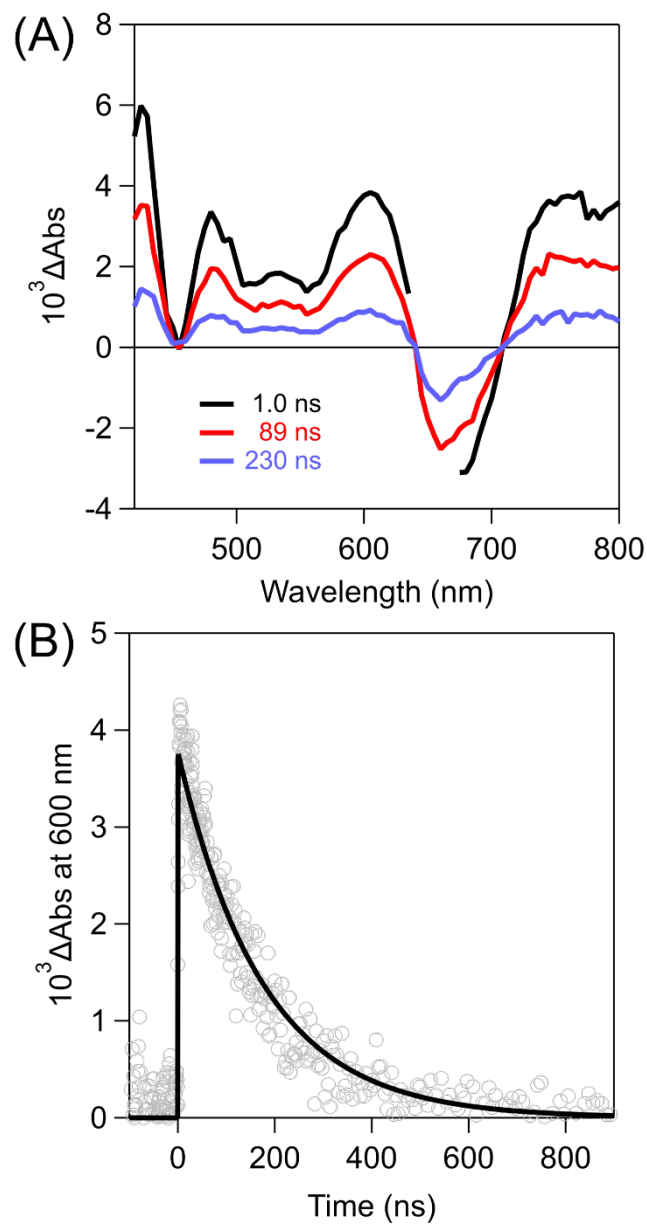


Fig. S14 (A) Picosecond transient absorption spectra (ps-TAS) and (B) corresponding time profile of Au₂₅(PET)₁₈ in Ar-saturated toluene ($\lambda_{\text{ex}} = 650$ nm) at room temperature (298 K). The triplet lifetime of Au₂₅(PET)₁₈ was determined to be 160 ns by single-exponential fitting. Measurements were performed at room temperature (298 K).

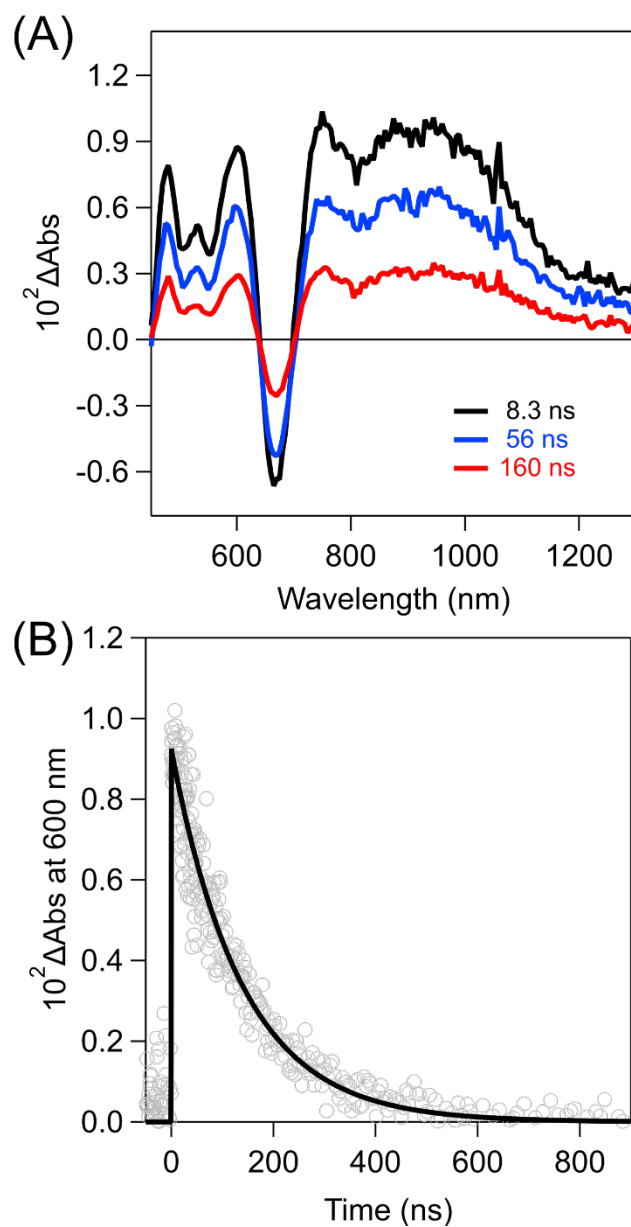


Fig. S15 (A) Picosecond transient absorption spectra (ps-TAS) and (B) corresponding time profile of $\text{Au}_{25}(\text{PET})_{18}$ in Ar-saturated toluene ($\lambda_{\text{ex}} = 355 \text{ nm}$) at room temperature (298 K). The triplet lifetime of $\text{Au}_{25}(\text{PET})_{18}$ was determined to be 160 ns by single-exponential fitting. Measurements were performed at room temperature (298 K).

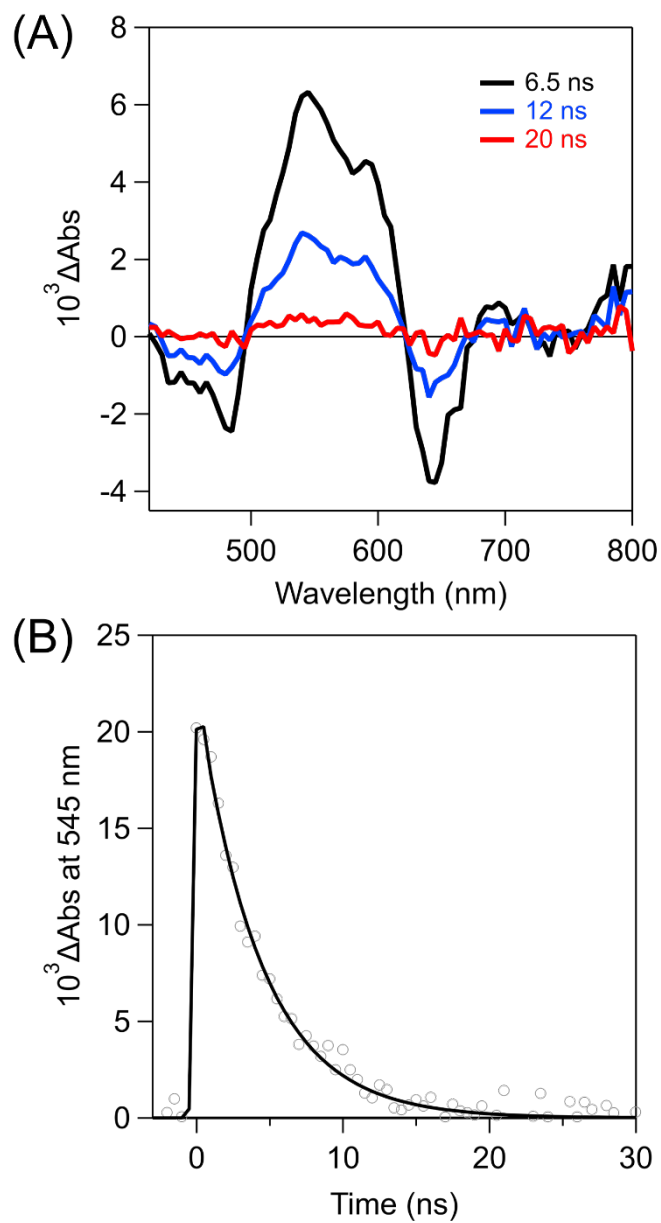


Fig. S16 (A) Picosecond transient absorption spectra (ps-TAS) and (B) corresponding time profile of $\text{Au}_{38}(\text{PET})_{24}$ in toluene ($\lambda_{\text{ex}} = 650 \text{ nm}$) at room temperature (298 K). The triplet lifetime of $\text{Au}_{38}(\text{PET})_{24}$ was determined to be 5.0 ns by single-exponential fitting. Measurements were performed at room temperature (298 K).

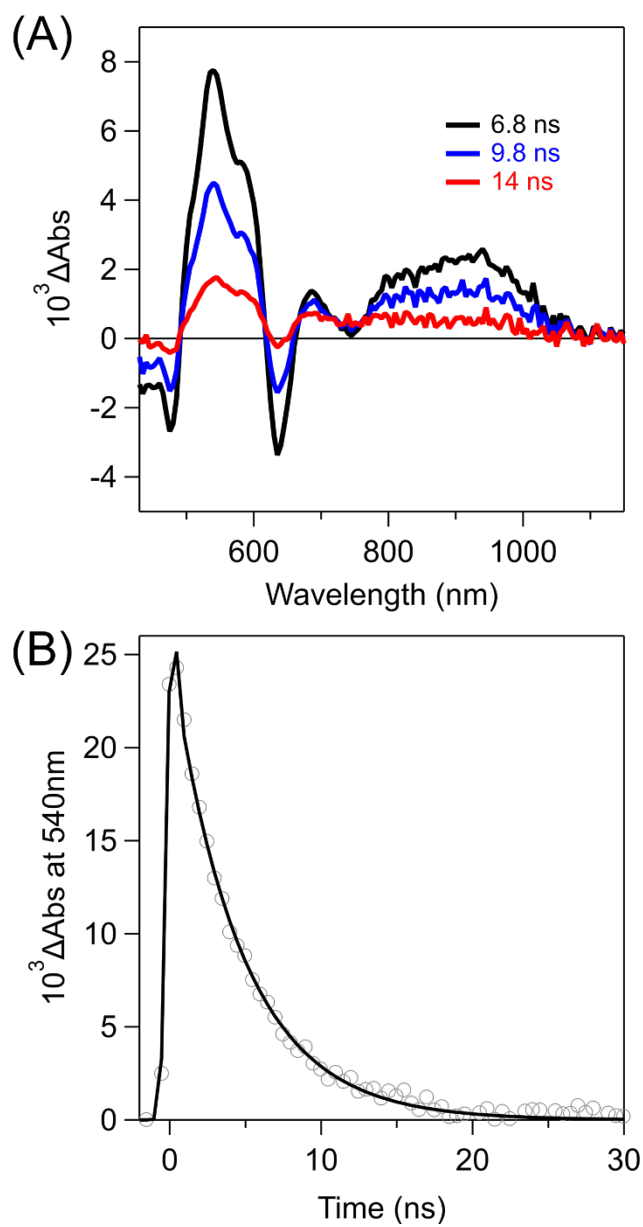


Fig. S17 Picosecond transient absorption spectra (ps-TAS) and corresponding time profile of Au₃₈(PET)₂₄ in toluene ($\lambda_{\text{ex}} = 355$ nm) at room temperature (298 K). The triplet lifetime of Au₃₈(PET)₂₄ was determined to be 5.0 ns by single-exponential fitting. Measurements were performed at room temperature (298 K).

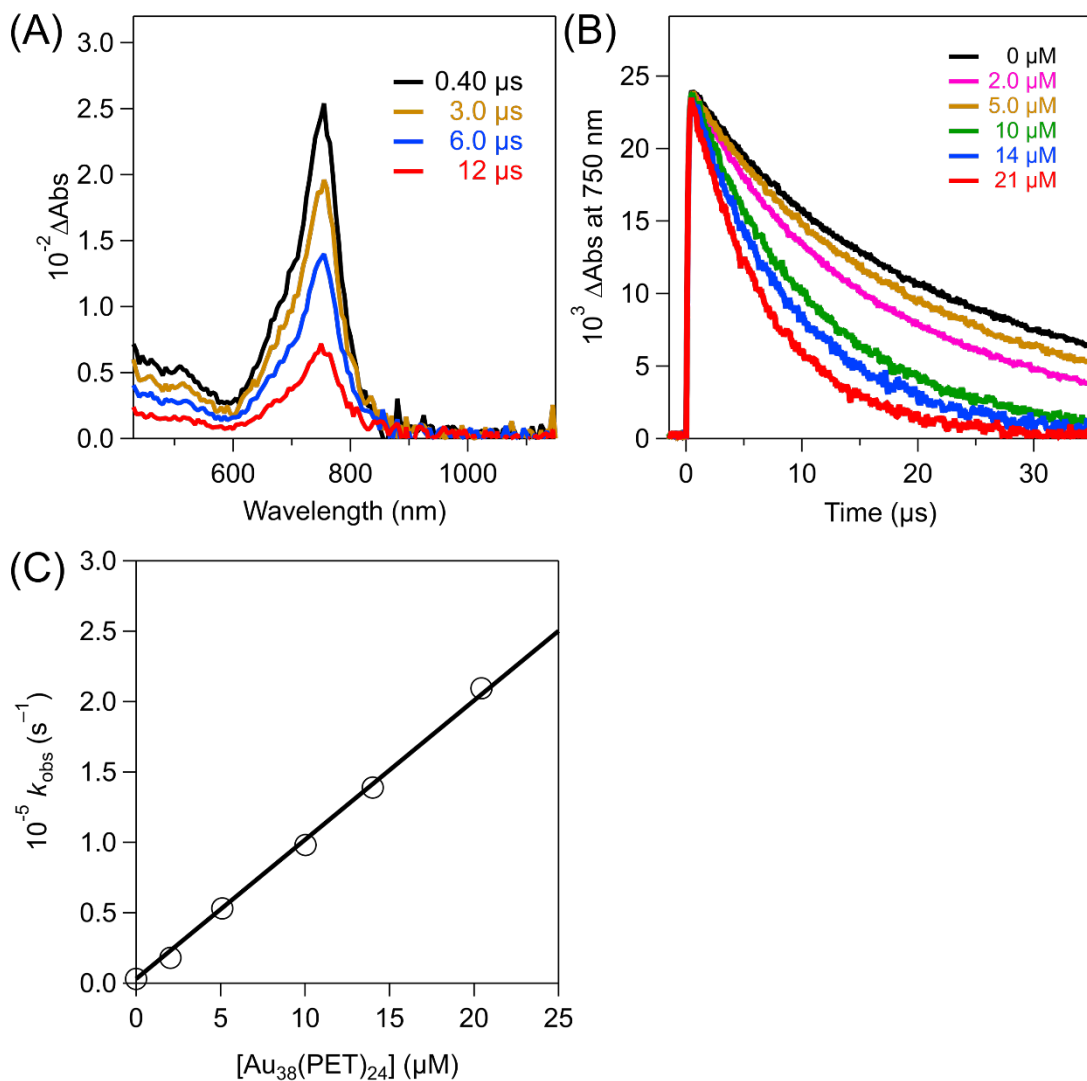


Fig. S18 (A) ps-TAS of C₆₀ (260 μM) in the presence of Au₃₈(PET)₂₄ (37 μM) excited at 355 nm in toluene (298 K). (B) The corresponding time profiles at 750 nm in the presence of different concentrations of Au₃₈(PET)₂₄. (C) Pseudo-first order plot of k_{obs} monitored at 750 nm versus concentrations of Au₃₈(PET)₂₄. The second-order rate constant is consequently estimated to be $9.9 \times 10^9 \text{ M}^{-1} \text{ s}^{-1}$.

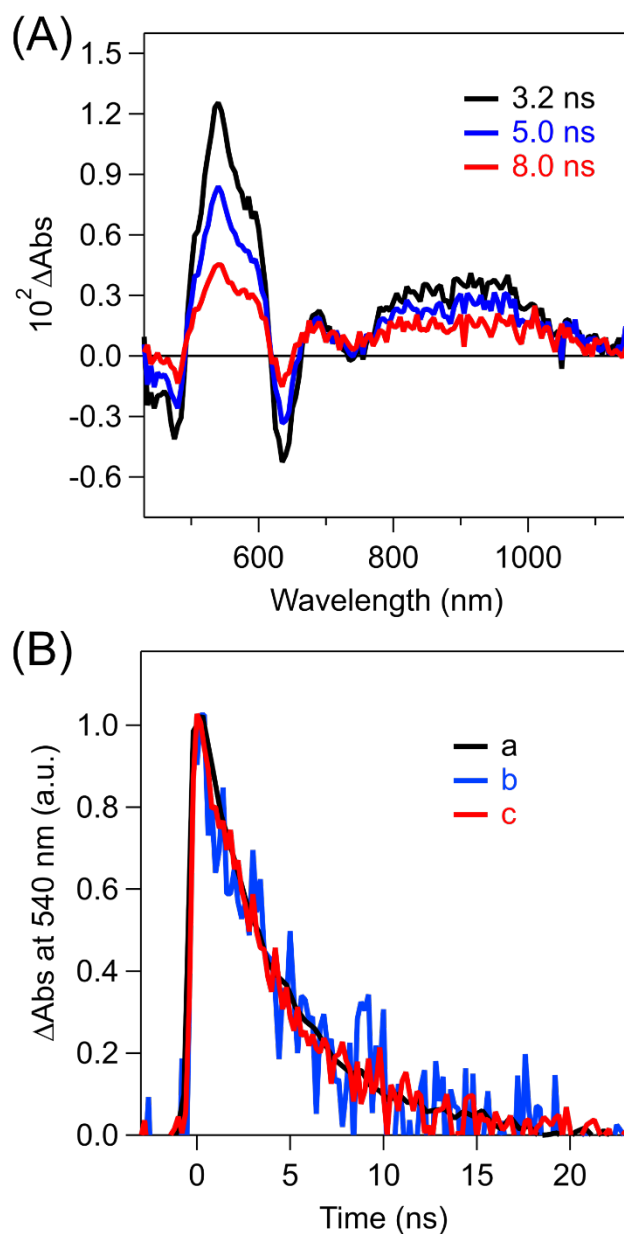


Fig. S19 (A) ps-TAS of $\text{Au}_{38}(\text{PET})_{24}$ in O_2 -saturated toluene ($\lambda_{\text{ex}} = 355 \text{ nm}$) at room temperature (298 K). (B) The corresponding time profiles of absorption at 540 nm in (a) Ar-saturated toluene, (b) air-saturated toluene and (c) $^3\text{O}_2$ -saturated toluene. These results indicated no quenching of $^3\text{Au}_{38}(\text{PET})_{24}^*$ with increasing the concentrations of $^3\text{O}_2$.

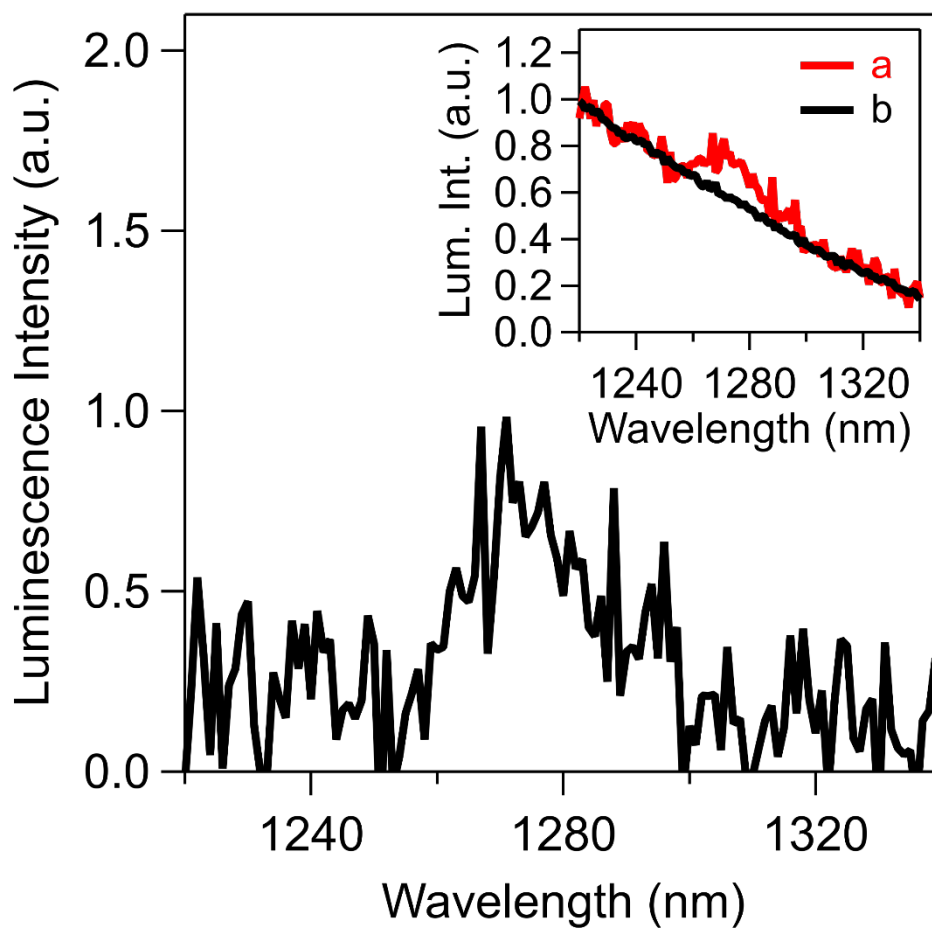


Fig. S20 A luminescence differential spectrum of $\text{Au}_{25}(\text{PET})_{18}$ in $^3\text{O}_2$ -saturated toluene at room temperature (298 K). The inset shows the parent luminescence spectra of $\text{Au}_{25}(\text{PET})_{18}$ in (a) $^3\text{O}_2$ -saturated and (b) Ar-saturated toluene solutions. $\lambda_{\text{ex}} = 650$ nm.

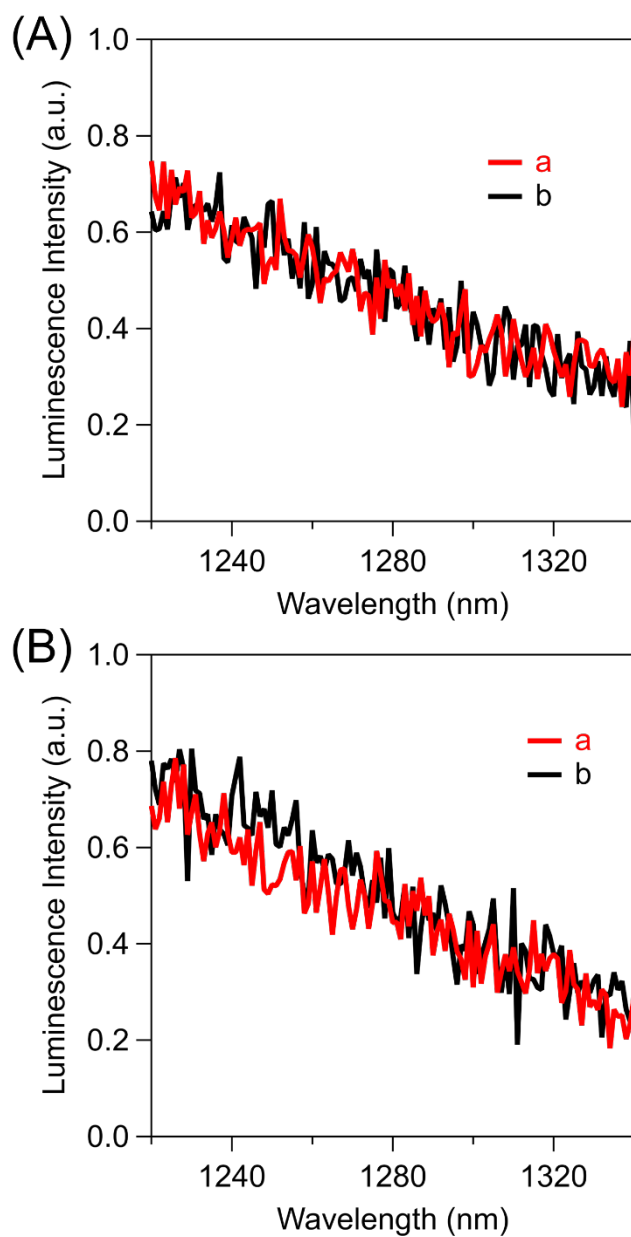


Fig. S21 (A) Normalized $^1\text{O}_2$ luminescence spectra of $\text{Au}_{38}(\text{PET})_{24}$ in (a) $^3\text{O}_2$ -saturated and (b) Ar-saturated toluene solutions ($\lambda_{\text{ex}} = 350$ nm) at room temperature (298 K). (B) Normalized $^1\text{O}_2$ luminescence spectra of $\text{Au}_{38}(\text{PET})_{24}$ in (a) $^3\text{O}_2$ -saturated and (b) Ar-saturated toluene solutions ($\lambda_{\text{ex}} = 650$ nm). These results agree well with no T-TEnT from $^3\text{Au}_{38}(\text{PET})_{24}^*$ to $^3\text{O}_2$ (See: Fig. S19).

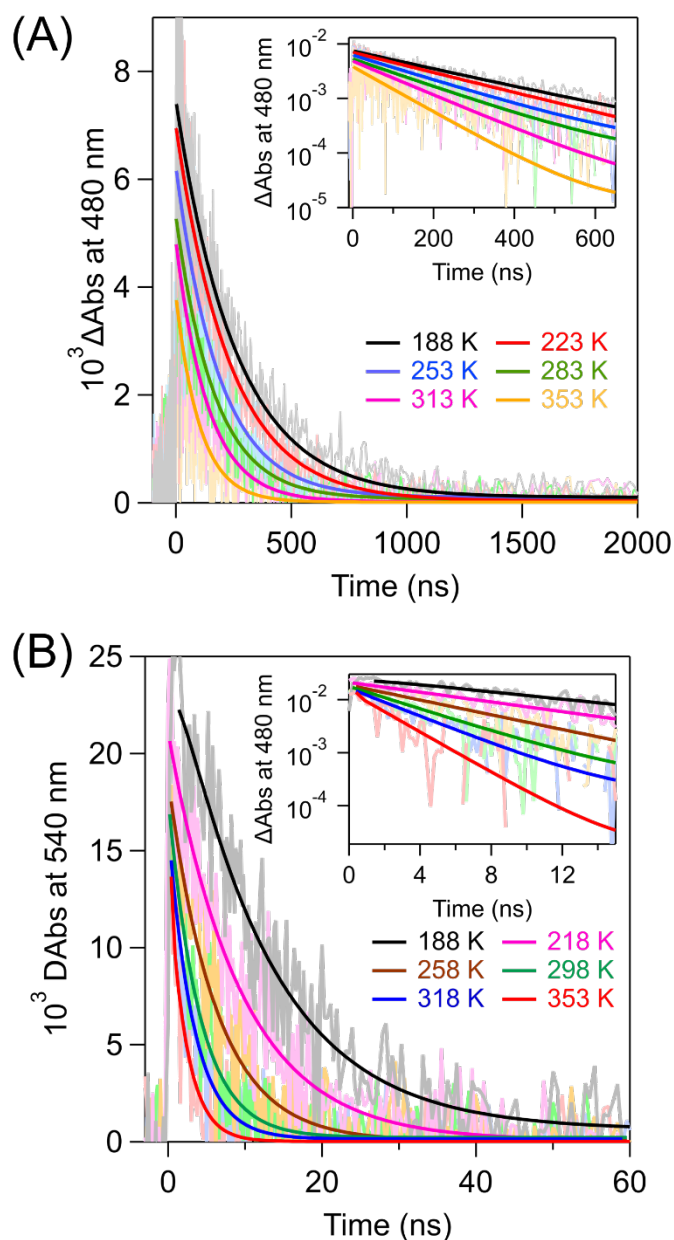


Fig. S22 (A) Temperature-dependent corresponding time profiles of ${}^3\text{Au}_{25}(\text{PET})_{18}^*$ at 480 nm in toluene using picosecond transient absorption measurements ($\lambda_{\text{ex}} = 355$ nm). The inset shows the y-axis changed from a linear scale to a logarithmic scale. (B) Temperature-dependent corresponding time profiles of ${}^3\text{Au}_{38}(\text{PET})_{24}^*$ at 540 nm in toluene at different temperatures using picosecond transient absorption measurements ($\lambda_{\text{ex}} = 355$ nm). The inset shows the y-axis changed from a linear scale to a logarithmic scale. In the inset showing ΔAbs on a logarithmic scale, the fitting curves for the time profiles at all temperatures are linear, which indicates that they are fitted with a single component.

Therefore, there is no transition process from T_1 to S_1 (RISC) for $Au_{25}(PET)_{18}$ and $Au_{38}(PET)_{24}$.

Additionally, the RISC process should be negligible considering the S_1 - T_1 gap (~ 0.3 eV) of $Au_{25}(PET)_{18}$. The transition probability from T_1 to S_1 at room temperature (298 K) can be calculated as follows.

$$\exp[-(\Delta E_{S-T}/(RT))] = \exp[-(0.3 \times 96500)/(8.31 \times 298)] = 8.4 \times 10^{-6}$$

This value strongly indicates that the RISC process does not occur at room temperature.

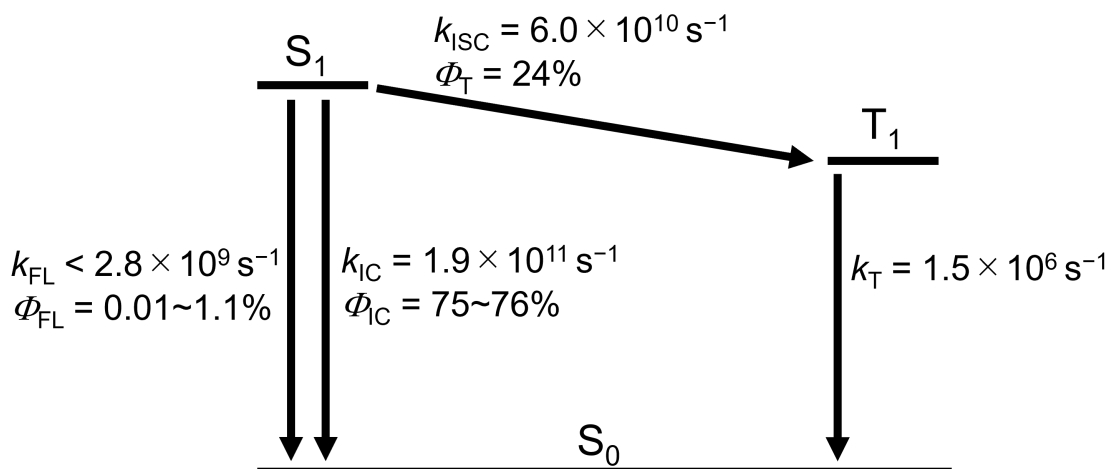


Fig. S23 The summarized Jablonski diagram of $\text{Au}_{25}(\text{PET})_{18}$ based on the previous and this works. k_{FL} : fluorescence emission rate constant, k_{ISC} : intersystem crossing rate constant, k_{IC} : internal conversion rate constant, k_T : triplet recombination rate constant, Φ_{FL} : fluorescence emission quantum yield,^{7,8} Φ_T : triplet quantum yield (this work), Φ_{IC} : internal conversion quantum yield (this work). The k_T was determined by the triplet decay lifetime of $\text{Au}_{25}(\text{PET})_{18}$ by ps-TAS of (160 ns as shown in Figs. S14 and S15).

The calculation of the Φ_T value (24%) of $\text{Au}_{25}(\text{PET})_{18}$ was discussed above (also see: Table 1 in the text). The Φ_{FL} values of $\text{Au}_{25}(\text{PET})_{18}$ were already reported in the range from 0.01 to 1.1% according to the previous works.^{7,8} Therefore, the Φ_{IC} value was calculated as follows (e.q. S2).

$$\Phi_{IC} = 1 - \Phi_{FL} - \Phi_{ISC} \quad (\text{eq. S2})$$

Then, the rate constants for k_{ISC} , k_{IC} and k_{FL} were accordingly estimated from the following equations (e.q. S3).

$$k_{FL} = \Phi_{FL} \cdot \tau_s^{-1}, k_{ISC} = \Phi_T \cdot \tau_s^{-1}, k_{IC} = \Phi_{IC} \cdot \tau_s^{-1} \quad (\text{eq. S3})$$

The τ_s (4.0 ps) corresponding to the singlet lifetime was determined by fs-TAS (Fig. 1 and Table 1 in the text), and k_{ISC} and k_{IC} were also calculated by using τ_s and corresponding quantum yields such as the Φ_T and Φ_{IC} values. For example, the k_{FL} value is equivalent to or smaller than $2.8 \times 10^9 \text{ s}^{-1}$. This is much smaller than those of ISC and IC processes (Φ_T and Φ_{IC}).

Calculation Method for Triplet Quantum Yields by Using Singlet Oxygen Luminescence

The triplet quantum yield (Φ_T) of Au₂₅(PET)₁₈ was calculated as follows (eq. S1).

$$\Phi_T = \Phi_{\text{std}} \left(\frac{F_{\text{Au}_{25}(\text{PET})_{18}}}{F_{\text{std}}} \right) \left(\frac{1 - 10^{-\text{Abs}_{\text{std}}}}{1 - 10^{-\text{Abs}_{\text{Au}_{25}(\text{PET})_{18}}}} \right) \quad (\text{eq. S1})$$

where $F_{\text{Au}_{25}(\text{PET})_{18}}$ is the integrated emission intensity of singlet oxygen generated by T-T EnT from Au₂₅(PET)₁₈, F_{std} is the integrated emission intensity of singlet oxygen generated by T-T EnT from C₆₀ used as standard molecule, $\text{Abs}_{\text{Au}_{25}(\text{PET})_{18}}$ is the absorbance of Au₂₅(PET)₁₈ at the excitation wavelength ($\lambda_{\text{ex}} = 650$ nm) and Abs_{std} is the absorbance of C₆₀ at the excitation wavelength ($\lambda_{\text{ex}} = 650$ nm).

The Φ_T values for Au₂₅(PET)₁₈ using C₆₀ as the standard molecule are summarized in Tables S1 and S2. The reported Φ_T value (1.0) for C₆₀ was used.⁹

Table S2. The Φ_T values of Au₂₅(PET)₁₈ ($\lambda_{\text{ex}} = 650$ nm) for five different experiments using C₆₀ as a standard molecule

Entry	Abs of Au ₂₅ (PET) ₁₈	Abs of C ₆₀	Φ_T of Au ₂₅ (PET) ₁₈ (%)
1	0.1098	0.01682	22.36
2	0.0904	0.01454	24.38
3	0.1042	0.01573	25.27
4	0.1067	0.01502	21.77
5	0.1092	0.01619	27.11

Based on the above results, the Φ_T of Au₂₅(PET)₁₈ ($\lambda_{\text{ex}}: 650$ nm) was determined to be $24 \pm 2.2\%$.

Table S3. The Φ_T values of Au₂₅(PET)₁₈ ($\lambda_{\text{ex}} = 350$ nm) for five different experiments using C₆₀ as a standard molecule

Entry	Abs of Au ₂₅ (PET) ₁₈	Abs of C ₆₀	Φ_T of Au ₂₅ (PET) ₁₈ (%)
1	0.6991	0.4235	24.41
2	0.6695	0.4171	23.50
3	0.6746	0.4154	23.80
4	0.6920	0.472	26.02
5	0.6266	0.3817	22.38

Based on the above results, the Φ_T of Au₂₅(PET)₁₈ (λ_{ex} : 350 nm) was determined to be $24 \pm 1.8\%$.

Determination of the molar absorption coefficients of ${}^3\text{Au}_{25}(\text{PET})_{18}^*$ based on the previous report¹⁰

Estimation of the concentrations of singlet excited states

Concentration of the singlet excited states was calculated as follows. When the solution in a cuvette is irradiated by the pump laser, the fraction of light intensity transmitted (I/I_0) through a solution can be calculated (excitation wavelength: 650 nm):

$$I/I_0 = 1 - 10^{-A(650 \text{ nm})} = 1 - 10^{-0.160} = 0.308$$

Then,

$$\begin{aligned} \frac{\text{photons}}{\text{pulse}} &= \frac{\text{laser power}}{(\text{repetition rate}) \cdot (\text{energy per photon})} \\ &= \frac{5.0 \times 10^{-3} \text{ W}}{(1000 \text{ s}^{-1}) \cdot (3.73 \times 10^{-19} \text{ J})} \\ &= 2.68 \times 10^{12} \end{aligned}$$

$$V = \pi \cdot r^2 \cdot d = \pi \cdot (0.1 \text{ cm})^2 \cdot (0.2 \text{ cm}) \cdot (0.001 \text{ L cm}^{-3}) = 6.28 \times 10^{-6} \text{ L}$$

Based on these values, the concentration of initial excited states can be calculated:

$$\begin{aligned} [{}^1\text{S}^*] &= \frac{(\text{photons/pulse}) \cdot (I/I_0)}{N_A \cdot V} \\ &= \frac{(2.68 \times 10^{12}) \cdot (0.308)}{(6.02 \times 10^{23} \text{ mol}^{-1}) \cdot (1.27 \times 10^{-6} \text{ L})} \\ &= 1.09 \times 10^{-7} \text{ M} \end{aligned}$$

Considering the triplet quantum yield ($24 \pm 2.2\%$) of $\text{Au}_{25}(\text{PET})_{18}$, the molar concentration of the triplet excited state of $\text{Au}_{25}(\text{PET})_{18}$ is $2.62 \times 10^{-7} \text{ M}$. From the value of $\Delta\text{Abs} = 0.00786$ in fs-TAS at 600 nm and the concentration of triplet excited states for $\text{Au}_{25}(\text{PET})_{18}$, the molar absorption coefficient of triplet excited state for $\text{Au}_{25}(\text{PET})_{18}$ was determined to be $30,000 \text{ M}^{-1} \text{ cm}^{-1}$ at 600 nm.

Then, the ε_T values of $\text{Au}_{25}(\text{PET})_{18}$ at 485, 535, 580, 600, 670 and 755 nm were also calculated as follows.

Table S4. The ϵ_T values of $\text{Au}_{25}(\text{PET})_{18}$ at five different wavelengths

Wavelength, nm	485	535	580	600	670	755
ΔAbs	0.00751	0.00598	0.00699	0.00786	-0.00467	0.00648
$\epsilon_T, \text{M}^{-1} \text{cm}^{-1}$	29000	23000	27000	30000	-18000	25000

Finally, the ϵ_T values of $\text{Au}_{25}(\text{PET})_{18}$ were summarized in Fig. 4B in the text.

References

1. T. Nakagawa, K. Okamoto, H. Hanada and R. Katoh, *Opt. Lett.*, 2016, **41**, 1498-1501.
2. J. J. Snellenburg, S. Laptinok, R. Seger, K. M. Mullen and I. H. M. van Stokkum, *J. Stat. Softw.*, 2012, **49**, 1-22.
3. X. Kang, H. Chong and M. Zhu, *Nanoscale*, 2018, **10**, 10758-10834.
4. H. Qian, Y. Zhu and R. Jin, *ACS Nano*, 2009, **3**, 3795-3803.
5. Z. Wu, J. Suhan and R. Jin, *J. Mater. Chem.*, 2009, **19**, 622-626.
6. P. N. Day, R. Pachter, K. A. Nguyen and R. Jin, *J. Phys. Chem. A*, 2019, **123**, 6472-6481.
7. Z. Wu and R. Jin, *Nano Lett.*, 2010, **10**, 2568-2573.
8. Z. Liu, Y. Li, E. Kahng, S. Xue, X. Du, S. Li and R. Jin, *ACS Nano*, 2022, **16**, 18448-18458.
9. D. K. Palit, A. V. Sapre, J. P. Mittal and C. N. R. Rao, *Chem. Phys. Lett.*, 1992, **195**, 1-6.
10. T. Sakuma, H. Sakai, Y. Araki, T. Mori, T. Wada, N. V. Tkachenko and T. Hasobe, *J. Phys. Chem. A*, 2016, **120**, 1867-1875.